PNAS RESEARCH ARTICLE | NEUROSCIENCE

EphB2-dependent prefrontal cortex activation promotes long-range social approach and partner responsiveness

Li-Na He[a,b], Si Chen[a,b], Qi Yang[a,b], Zheng Wu[a], Zheng-Kai Lao[a,b], Chang-Fei Tang[a,b], Jiao-Jiao Song[a], Xian-Dong Liu[c], Jiangteng Lu[a,b], Xiao-Hong Xu[d], Jin-Jin Chen[a], Tian-Le Xu[a,b], Suya Sun[c,1], and Nan-Jie Xu[a,b,e,f,1]

Edited by Richard Huganir, Johns Hopkins University School of Medicine, Baltimore, MD; received November 22, 2022; accepted January 15, 2023

Social behavior starts with dynamic approach prior to the final consummation. The flexible processes ensure mutual feedback across social brains to transmit signals. However, how the brain responds to the initial social stimuli precisely to elicit timed behaviors remains elusive. Here, by using real-time calcium recording, we identify the abnormalities of EphB2 mutant with autism-associated Q858X mutation in processing long-range approach and accurate activity of prefrontal cortex (dmPFC). The EphB2-dependent dmPFC activation precedes the behavioral onset and is actively associated with subsequent social action with the partner. Furthermore, we find that partner dmPFC activity is responsive coordinately to the approaching WT mouse rather than Q858X mutant mouse, and the social defects caused by the mutation are rescued by synchro-optogenetic activation in dmPFC of paired social partners. These results thus reveal that EphB2 sustains neuronal activation in the dmPFC that is essential for the proactive modulation of social approach to initial social interaction.

social behavior | prefrontal cortex | EphB2 | autism

Significance

Social behavior undergoes sophisticated sequential processes that are associated functionally in the brain, but little is known how the social action is proactive determined. The study reveals that EphB2 serves as a crucial molecule, by using knockin mice with autism-associated point mutation, in sustaining long-range approach toward the partner. The EphB2-dependent neuronal activity is accurately induced in dmPFC preceding the approach onset and is correlated coherently with the responsive activation in the partner's brain. The study thus identifies a key molecular function in dmPFC required to elicit social behavior, which may help unlock the secrets of the autism brain for behavioral disorders.

Social behavior is critical for survival and prosperity in most group animals. Individuals interacting with their social partner exhibit a wide range of behavioral exhibitions, which are successively represented as detection, approach, sniffing, and consummation (1, 2). Social interaction requires the perception and integration of social stimuli through a complex process involving attention, memory, motivation, and emotion (3, 4). It also needs to combine with the inner physiological state of the self to guide a behavioral response adapted to a particular situation (5–7). The disruption of social priming or social information processing might lead to behavioral disorders characterized by social dysfunction, such as autism, schizophrenia, and depression.

Social information processing is initiated by sensory input via visual, olfactory, and auditory centers, and it transmits the signals into prefrontal cortex, temporal lobe cortex, and amygdala for the development of the individual preference (8–10). In the past decade, the process has been studied by using molecular and cellular approaches and neuroimaging tools for various aspects of social behavior and social cognition (9). Accumulating evidence indicates that any particular social behavior of a species is the result of genetic, epigenetic, and environmental factors. In particular, a series of molecules involved in the synaptic function of cortical neurons, such as Shank family (11), Nlgn family (12), and Cntnap2 (13) that have been identified in the social disorders, are highly correlated with the multisource integration of cues for social interactions. Considering the inherent complexity of social behaviors, the neural basis underlying these behavioral disorders is still not well understood.

EphB2 receptor has been found, with de novo mutations, associated with autism by whole-exome sequencing of peripheral blood from humans (14, 15). Although extensive evidence indicates that EphB2 plays key roles in regulating synaptic plasticity and cognitive behaviors (16), including social recognition memory (17), social isolation-induced memory forgetting (18), and autism-associated repetitive behaviors (19), it remains elusive whether the autism-associated EphB2 mutations account for the behavioral disorders including defects in perception and integration of social cues needed for sociability. In the current study, we observed that EphB2 mutant with autism-associated point mutation Q858X exhibited stereotyped approach and consequent social dysfunction that was attributable to disrupted neuronal activity in dorsal medial prefrontal cortex (dmPFC), an integrative center for both approach and sniffing epochs, which was restored by specific overexpression of EphB2 in dmPFC. Importantly, we found that the dmPFC activity of the partner was also responsive timely to the approaching mouse, and the interbrain correlation in activity requires EphB2. Furthermore, the social deficits in Q858X mutant could be rescued by synchro-optogenetic activation of dmPFC. Our results thus reveal a proactive mechanism in the dmPFC underlying the long-range approach for appropriate social behavior.

Author contributions: S.S. and N.-J.X. designed research; L.-N.H., S.C., Q.Y., Z.W., and J.-J.S. performed research; L.-N.H., Q.Y., Z.-K.L., and C.-F.T. analyzed data; X.-D.L., J.L., X.-H.X., J.-J.C., and T.-L.X. supervised research; and L.-N.H., S.S., and N.-J.X. wrote the paper.

The authors declare no competing interest.

This article is a PNAS Direct Submission.

[1]To whom correspondence may be addressed. Email: sunsuya@shsmu.edu.cn or xunanjie@sjtu.edu.cn.

This article contains supporting information online at https://www.pnas.org/lookup/suppl/doi:10.1073/pnas.2219952120/-/DCSupplemental.

Published February 21, 2023.

Results

EphB2 Mutant Shows Impaired Social Approach and Sniffing. To identify whether the behavioral property of animals with their partners is impaired by autism-associated de novo mutations in *EPHB2* gene, we generated two knockin mouse lines, with point mutation Q858X and G900S, respectively (*SI Appendix*, Figs. S1 and S2), and examined their behaviors in a three-chamber paradigm to probe their sociability (*SI Appendix*, Fig. S3). We found that the Q858X mutant and $EphB2^{-/-}$ (EphB2 KO) mice showed much lower sociability index from juvenile stage to adulthood (*SI Appendix*, Fig. S3 *A* and *B*). The impaired social behaviors observed in Q858X mutant mice might be attributable to the truncated EphB2 (Q858X) that was expressed in a low level and lacking of tyrosine phosphorylation (*SI Appendix*, Figs. S1*E* and S2). This was distinct to our observation in $Lnx1^{-/-}$ mice, in which low-level expression of EphB2 results in only defective social memory (17). In contrast, the G900S mutant mice behaved as normal as WT. We further tested these mice for a wide range of behaviors including social approach and sniffing, two consequent events prior to direct social contact (*SI Appendix*, Fig. S3 *C–F* and Movie S1). During either events, WT mice showed obvious partner preference compared with empty cage, which was abolished in either Q858X mutant or EphB2 KO mice but not in G900S mutant mice (*SI Appendix*, Fig. S3 *C–F*).

To further examine how two freely moving social partners react to each other, we performed a reciprocal social behavioral test, in which nose-to-nose contact for social sniffing could be clearly observed, and a transverse partition prevented aggressive behavior (Fig. 1*A*). We found that WT mice displayed an obvious preference for interaction area with their partners, while the Q858X (refer to as EphB2 KI) mice exhibited less time in interaction area (Fig. 1*B*). Moreover, we analyzed each single social approach or sniffing event upon nose-to-nose interacting with the partner and observed that WT mice spent longer time in each approach or sniffing epoch than EphB2 KI mice (Fig. 1*C*). To clarify whether the duration in each approach is related to the distance from the social subject to partner, we measured the nasal tip distance across social animals when the social approach was initiated (Fig. 1*D*), and observed that the distance of WT mice to trigger approach was remarkably longer than that of EphB2 KI mice and correlated with duration of each approach (Fig. 1 *E* and *F*). According to the mean approaching time of WT and KI mice as about 2 s and 1 s, respectively, we classified the social behavioral events into four categories of duration, 0 to 1.5 s, 1.5 to 3 s, 3 to 4.5 s, and over 4.5 s. We observed that WT mice represented all four categories, whereas the Q858X mutation resulted in reduced types, leaving only types I and II (Fig. 1*G*). Notably types III and IV showed longer distance from subject to partner compared with types I and II, while the approach epochs with the longer distance were completely disrupted in EphB2 KI mice (Fig. 1*H*). Moreover, to explore whether the type of approach related to social sniffing, we plotted the percentage of types I + II or types III + IV versus sniffing duration, and found that the proportion of types III + IV was positively correlated with the sniffing duration (Fig. 1*I*). Q858X mutation eliminated the correlation during social behavior (Fig. 1*I*). In addition, we examined the visual and olfactory functions of EphB2 KI mice and found no significant difference compared to WT mice (*SI Appendix*, Fig. S4). These observations suggest that the timing of dynamic social approach is associated with mouse sociability, and Q858X mutation impedes the long-range approach ability of mice that may result in social dysfunction.

EphB2 Mediates Accurate Activation of dmPFC Neurons during Reciprocal Social Behavior. We then asked which brain regions were mainly affected by the Q858X mutation during social interaction. To explore the activated brain regions responding to social cues, we employed targeted recombination in active populations (TRAP2) strategy with $Fos^{2A\text{-}iCreER/+}$ mice crossed with a floxed tdTomato reporter mouse line (AI9) to label specific neurons that were activated by social interaction with partners, which could be reflected through the expression of $tdTomato^{+}$ in whole-brain neurons (*SI Appendix*, Fig. S5*A*). We screened for EphB2-enriched brain regions with $tdTomato^{+}$ neurons increased during social interactions and found that EphB2 KI mice exhibited eliminated $tdTomato^{+}$ neurons in prefrontal cortex (PFC) and hippocampal DG region among a large number of activated brain regions with $tdTomato^{+}$ signals (*SI Appendix*, Fig. S5*B*). Given EphB2 expression is highly enriched in dmPFC neurons unlike other subtypes such as EphB1 and EphB3, and EphB2 KI mice had a greater effect on the PFC neuronal activity under the social paradigm (*SI Appendix*, Figs. S5–S7), we examined the functional consequence of Q858X mutation on synaptic transmission in dmPFC through synaptic protein immunoblotting and whole-cell patch clamp recording (*SI Appendix*, Fig. S8). The western blot analysis revealed a decreased protein levels of the AMPARs and NMDARs in the EphB2 KI mice (*SI Appendix*, Fig. S8*A*). We also observed reduced action potential and slower post-hyperpolarization potential in response to depolarizing pulse that was recorded in PFC neurons from the EphB2 KI mice (*SI Appendix*, Fig. S8 *B* and *C*), while the ratio of evoked AMPAR/NMDAR between WT and EphB2 KI mice remained unchanged (*SI Appendix*, Fig. S8*D*). These results indicate that the Q858X mutation disrupts the excitatory synaptic transmission of neurons in the dmPFC.

We then monitored the in vivo neuronal activity of freely moving mice during reciprocal social interaction through injection of AAV-Syn-GCaMP6s in dmPFC and combined with fiber photometry for calcium signal recording (Fig. 2 and *SI Appendix*, Fig. S9). Firstly, we found that segregating the mice from their social partners via a black opaque panel significantly reduced the frequency and area under curve of calcium signal in WT mice, while the signal in EphB2 KI mice kept at a lower level (*SI Appendix*, Fig. S9). We then analyzed in detail the changes of dmPFC neuronal activity in each single social approach or sniffing event in reciprocal social interaction, and found that the calcium signal was dramatically increased in WT mice during either approach or sniffing epochs, while they differed in the intensity and dynamics of calcium waves (Fig. 2*A*). The area under curve and peak value of calcium signal revealed that neuronal activities of approach increased more dramatic than that of sniffing (Fig. 2 *A* and *B*). We further analyzed the responding time of dmPFC neurons within approach and sniffing epoch respectively, and observed that calcium signals within approach epochs preceded the behavior onset for about 2 s, while the calcium signals of sniffing epochs rose 1 s right after the behavior onset (Fig. 2*C*), indicating that dmPFC neurons might be dual-responsive to both initiating of social interaction (approach) and processing of information about other agents (sniffing). In contrast, EphB2 KI mice exhibited significantly decreased calcium peak value and duration in either approach or sniffing stages compared to WT mice (Fig. 2 *A* and *C*). These results indicate that Q858X mutation impairs the response of dmPFC within both approach and sniffing epochs.

To further investigate how dmPFC activity in subject mice is elicited, we recorded the timed calcium signals upon approach or sniffing to calculate the time difference of the two calcium peaks, and plotted these data versus duration from approach onset to

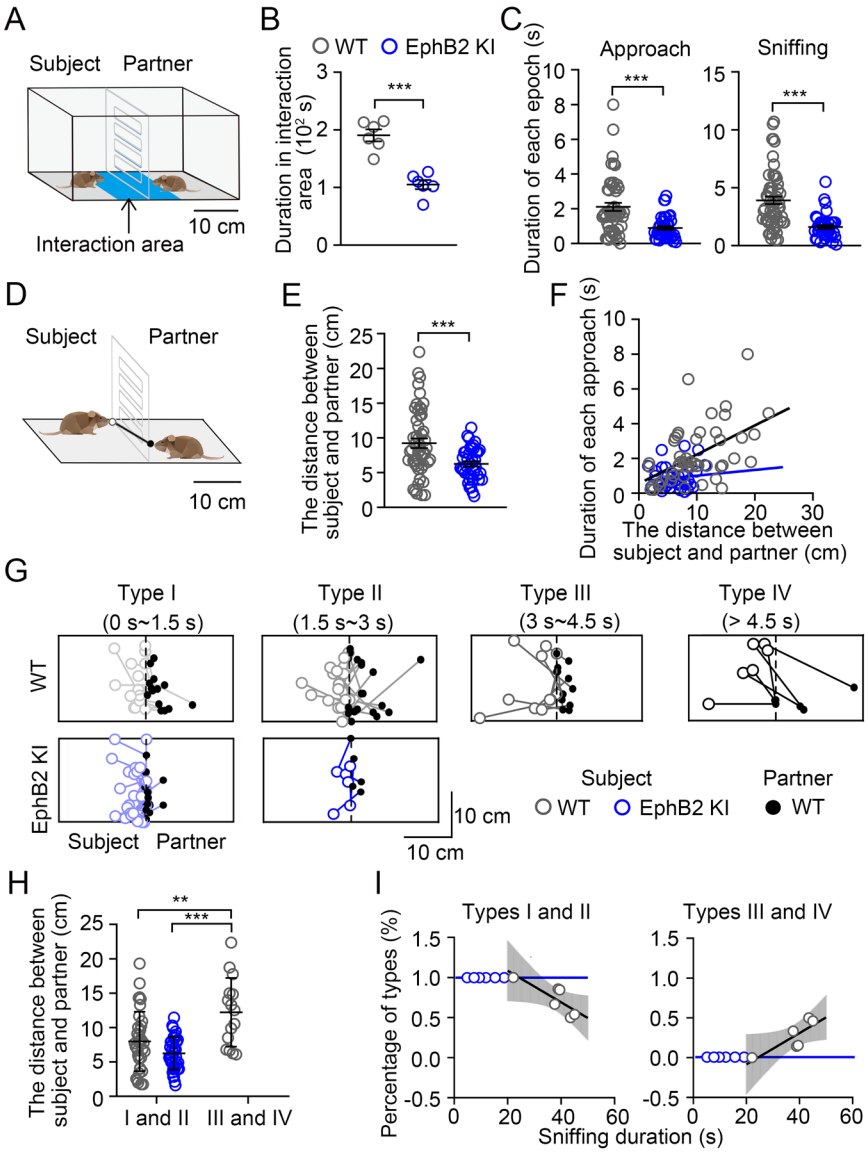

Fig. 1. Impaired Social Approach and Sniffing in EphB2 KI Mice. (*A*) Schematic of the reciprocal social interaction paradigm. (*B*) Duration in interaction area was calculated in WT and EphB2 KI groups. (*C*) Duration of each approach (*Left*) or sniffing (*Right*) was examined in two groups. (*D*) Schematic of the distance from subject to partner. (Scale bar: 10 cm). (*E*) The distance across social individuals was measured in all two groups of mice. (*F*) Correlation between the distance and the approach time. WT, R = 0.52, $P < 0.0001$; EphB2 KI, R = 0.12, $P = 0.47$; (*G*) Distance traces of WT or EphB2 KI mice during reciprocal social interaction. [Scale bar: 10 cm (vertical) × 10 cm (horizontal).] Example trace: Black from light to dark represents various time intervals of WT mice: 0 s ~ 1.5 s, 1.5 s ~ 3 s, 3 s ~ 4.5 s, >4.5 s (*Top*); Blue from light to dark represents various time intervals of EphB2 KI mice: 0 s ~ 1.5 s, 1.5 s ~ 3 s (*Bottom*). (*H*) Per-type plot of distance was calculated in all two groups of mice. (*I*) Correlation between the percentage of types I and II (*Left*) or that of types III and IV (*Right*) and the sniffing duration in two groups of mice. *Left*: WT, R = 0.81, $P = 0.049$; EphB2 KI, R = 1; *Right*: WT, R = 0.81, $P = 0.049$; EphB2 KI, R = 1. n = 58 reciprocal social interaction events from six mice for WT group and n = 42 reciprocal social interaction events from six mice for EphB2 KI group. Data are presented as mean ± SEM. $^*P < 0.05$; $^{**}P < 0.01$; $^{***}P < 0.001$; two-tailed *t* test (*B*, *C*, and *E*) and two-way ANOVA with Tukey's multiple comparisons test (*H*).

sniffing. We found a significant correlation between the timing of calcium signal and approach duration, indicating that approach epoch is capable of triggering accurate neuron activities precisely in the dmPFC brain region (Fig. 2*D*). In contrast, the data from EphB2 KI mice were restrictively distributed in a small range, exhibiting much shorter duration from approach to sniffing in either calcium signal or behaviors (Fig. 2*D*), which was consistent with behavioral exhibitions (Fig. 1). We then classified and analyzed calcium signals according to the four categories of approach duration (Fig. 1*G* and 2*E*), and observed that in WT mice the category of calcium signal patterns exhibited more diverse waveforms, showing a dynamic timing of dmPFC signal, consistent with all approach types I to IV (Fig. 2 *E* and *F*). In contrast, the Q858X mutation resulted in limited calcium signaling types, leaving only types I and II (Fig. 2 *E* and *F*). The type I signal accounts for 86% of the total social contact events in EphB2 KI mice, exhibiting more similar calcium signal waveform (Fig. 2*F*). Moreover, we found that in WT mice the decay time and peak value of calcium signals for social approach in types III and IV were significantly higher than that in types I and II, while Q858X mutation abolished such changes in the calcium signals during approach epochs with only types I and II calcium signals left (Fig. 3 *G* and *H*). To investigate whether the amplitude of calcium signals was related to animals' ability for long-range approach, we plotted the peak value of approach/sniffing versus the distance from subject to partner, and found that the calcium peak in types III and IV was positively correlated with the approach distance, while the correlation was not found in types I and II (Fig. 2*I*). These observations reveal that

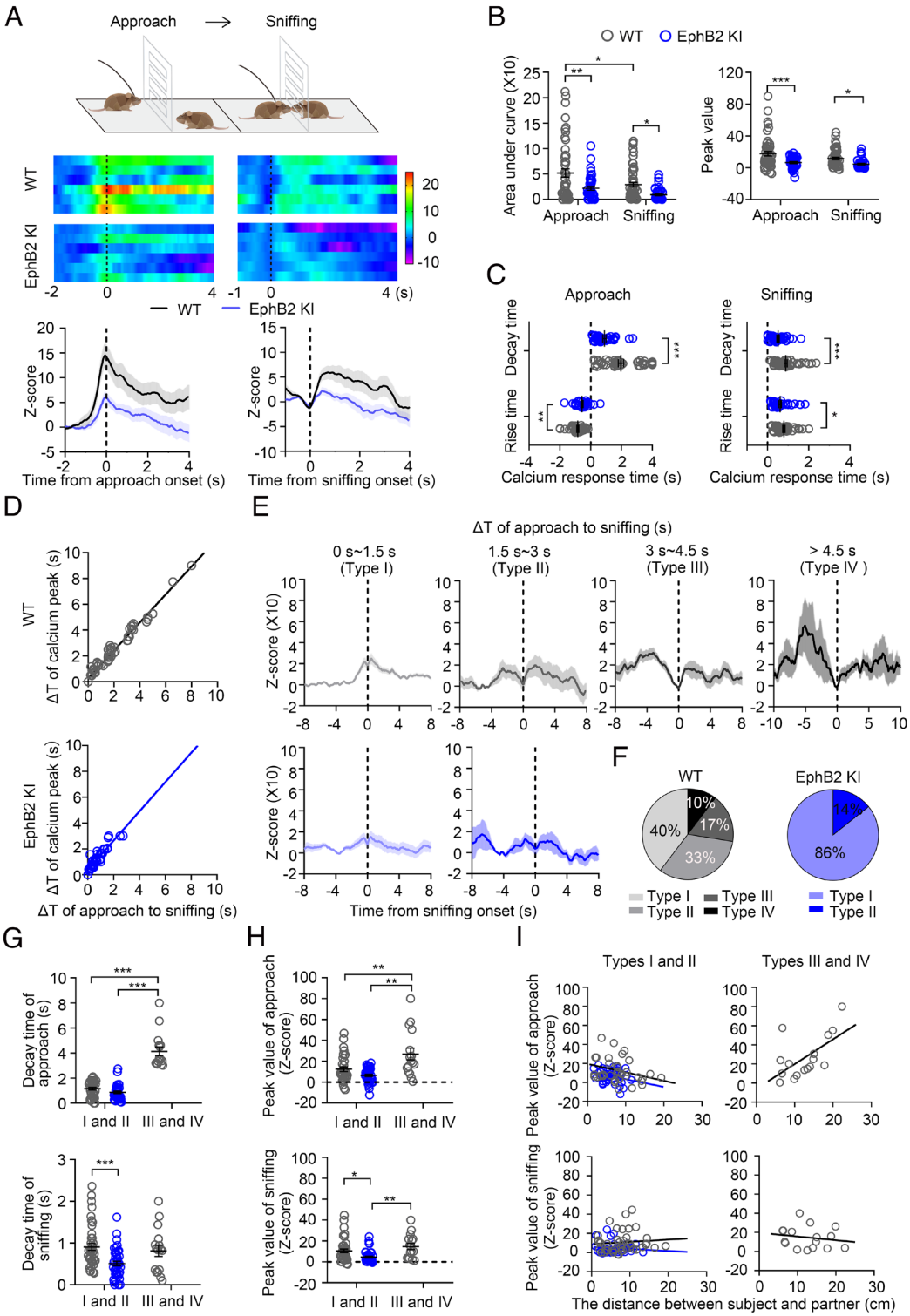

Fig. 2. dmPFC Neurons Show Hypoactivity during Reciprocal Social Interaction in EphB2 KI Mice. (*A*) Schematic illustrating the two social processes: social approach (*Top*, *Left*) and sniffing (*Top*, *Right*). Heat map illustrating the calcium response (Z-score) of dmPFC neurons in approach (*Middle*, *Left*) or sniffing (*Middle*, *Left*) events. Per-event plot of averaged calcium signals during approach (*Bottom*, *Left*) or sniffing (Bottom, *Right*) in WT and EphB2 KI mice. Solid line and the shaded regions are the mean ± SEM. (*B*) Quantification of area under Z-score curve (*Left*) or peak value (*Right*) in approach and sniffing events. (*C*) Quantification of raise time or decay time in approach (*Left*) and sniffing epochs (*Right*) in two groups of mice. (*D*) Scatterplots of the time difference between approach to sniffing and two calcium signal peaks. *Top*: WT mice, R = 0.98, $P < 0.0001$; *Bottom*: EphB2 KI mice, R = 0.92, $P < 0.001$. (*E*) Example trace: Black from light to dark represents various time intervals of WT mice: 0 s ~ 1.5 s, 1.5 s ~ 3 s, 3 s ~ 4.5 s, >4.5 s (*Top*); Blue from light to dark represents various time intervals of EphB2 KI mice: 0 s ~ 1.5 s, 1.5 s ~ 3 s (*Bottom*). (*F*) Pie graph showing the percentage distribution of various time intervals from approach to sniffing. *Left*, WT mice; *Right*, EphB2 KI mice. (*G*) Per-type plot of decay time of approach (*Top*) or sniffing (*Bottom*). (*H*) Per-type plot of peak value of approach (*Up*) or sniffing (*Bottom*). (*I*) Correlation between the distance of type I and II (*Left*) or that of type III and IV (*Right*) and the peak value of approach (*Top*) or sniffing (*Bottom*). Approach (*Top*): WT mice, R = 0.31, $P = 0.077$ (*Left*, types I and II); EphB2 KI mice, R = 0.27, $P = 0.093$ (*Left*, types I and II); WT mice, R = 0.6, $P = 0.014$ (*Right*, types III and IV). Sniffing (*Bottom*): WT mice, R= 0.093, $P = 0.56$ (*Left*, types I and II); EphB2 KI mice, R = 0.1, $P = 0.41$ (*Left*, types I and II); WT mice, R = 0.18, $P = 0.51$ (*Right*, types III and IV). n = 58 reciprocal social interaction events from six mice for WT group and n = 42 reciprocal social interaction events from six mice for EphB2 KI group. Data are presented as mean ± SEM. *$P < 0.05$; **$P < 0.01$; ***$P < 0.001$; two-way ANOVA with Tukey's multiple comparisons test.

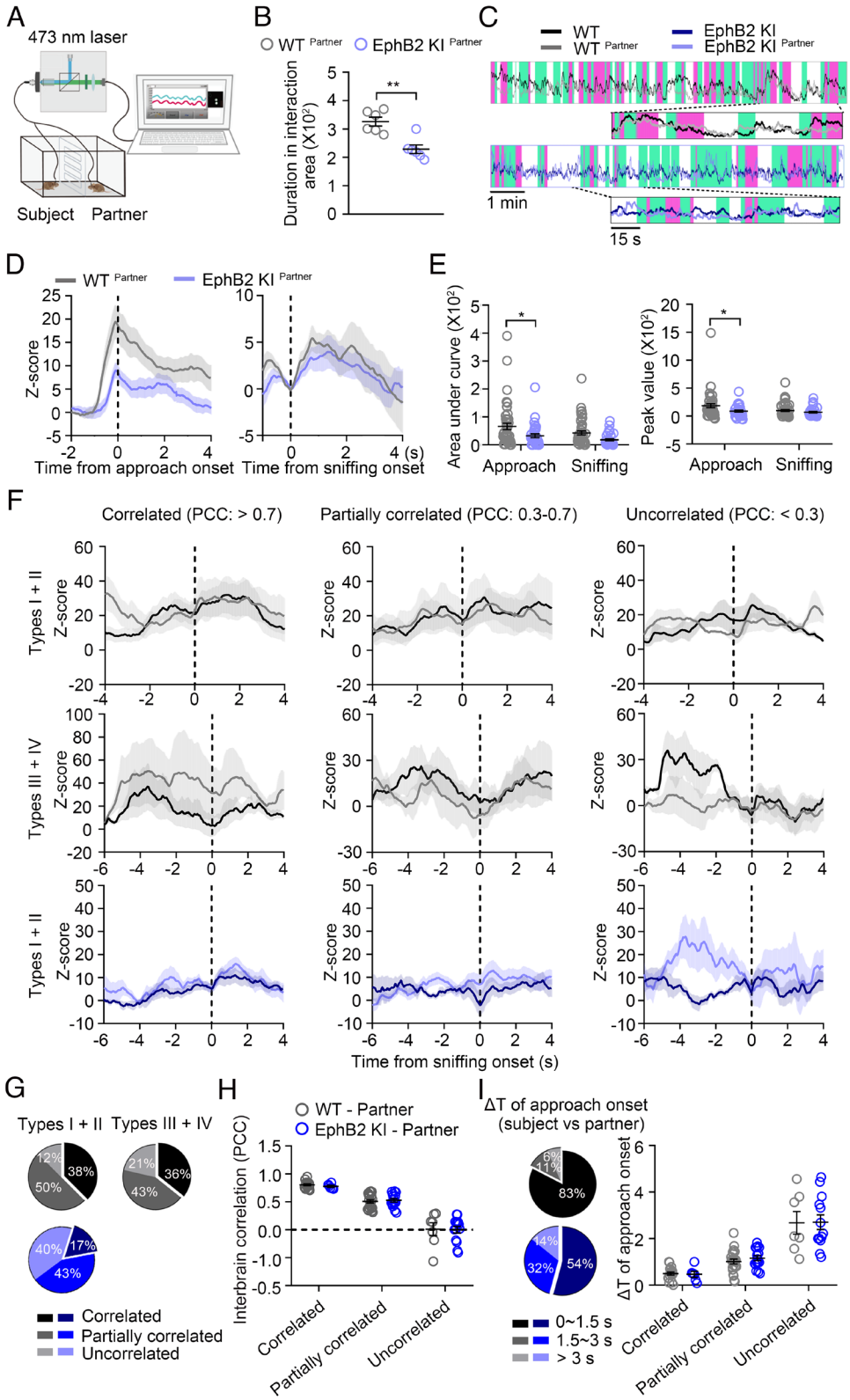

Fig. 3. EphB2 Q858X Mutation Disrupts Partner Responsiveness in dmPFC Activity. (*A*) Schematic representations of the procedure used to record calcium activity during reciprocal social interaction. (*B*) Duration in interaction area was analyzed in partners of WT or EphB2 KI mice. (*C*) Example calcium traces of dmPFC neurons during reciprocal social interaction cover with behavior annotations. White, Non-social phase; Green, Intermedial phase; Pink, Social phase. (*D*) Plot of averaged calcium signals of approach (*Left*) or sniffing (*Right*) events in partners of WT or EphB2 KI mice. Solid line and the shaded regions are the mean ± SEM. (*E*) Quantification of area under Z-score curve (*Left*) or peak value (*Right*) in approach and sniffing events for all two groups' partners. (*F*) Averaged calcium traces of dmPFC neurons between social individuals: correlated, partially correlated or uncorrelated are classed by the Pearson's correlation coefficient (PCC) for all types of two paired groups. (*G*) The proportion of correlated, partially correlated or uncorrelated under different types of approach. (*H*) Comparison of the interbrain correlations between subject and partner in the correlated, partially correlated or uncorrelated groups. (*I*) Pie graph showing the percentage distribution of time intervals from subject's approach to partner's approach (*Left*). Comparison the time intervals between subject and partner in different interbrain correlation (*Right*). n = 6 pairs for WT paired group and n = 6 pairs for EphB2 KI paired group, the number of partner mice was the same as that of the subjects. Data are presented as mean ± SEM. *P < 0.05; **P < 0.01; two-tailed t test (*B*) and two-way ANOVA with Tukey's multiple comparisons test (*E*).

dmPFC activity is closely related to the ability for long-range social approach, and Q858X mutation disrupts the diverse timing of PFC neuronal activation required for the ability.

Restoration of EphB2 in dmPFC Rescues Neuronal Activity for Social Approach. To explore whether selectively restoring EphB2 function in dmPFC neuron is sufficient to rescue social dysfunction and hypoactivity of dmPFC to approach, we overexpressed the full-length EphB2 into dmPFC of EphB2 KI mice through injecting AAV-Syn-EphB2-mCherry and AAV-Syn-GCaMP6s for the calcium signal recording during reciprocal social behavior (*SI Appendix*, Fig. S10*A*). We found that the EphB2 overexpression significantly increased the time spent in the interaction area and the duration of each social approach or sniffing (*SI Appendix*, Fig. S10 *B* and *C*). Furthermore, we found that EphB2 overexpressing group showed longer distance from social subject to partner compared to control EphB2 KI mice, and the correlation between the duration and the distance of approach was also improved (*SI Appendix*, Fig. S10 *D* and *E*). In EphB2 overexpressing group, number of type III social interaction was remarkably increased compared with that in types I and II, and the higher the proportion of type III reached, the longer the time of reciprocal social sniffing spent (*SI Appendix*, Fig. S10 *F* and *H*). We also observed the recused social behavior by three-chamber paradigm (*SI Appendix*, Fig. S11). These results suggest that overexpression of EphB2 protein in the dmPFC of EphB2 KI mice restores the ability of long-range approach to ensure that social behaviors function properly.

We then examined the activation of dmPFC neurons responding to reciprocal social interaction in EphB2 overexpressing mice (*SI Appendix*, Fig. S12). We found that overexpression of EphB2 in the dmPFC led to increased calcium amplitude in social approach epochs compared with EphB2 KI mice (*SI Appendix*, Fig. S12 *A*–*C*). Likewise, EphB2 overexpressing group exhibited earlier rise time and longer decay time for approach epochs (*SI Appendix*, Fig. S12 *D* and *E*), whereas these improved calcium signals were not seen in sniffing epochs (*SI Appendix*, Fig. S12 *A*–*D*). Consistent with behavioral results, we observed that the distribution of calcium signals in correlation analysis was reversed by EphB2 overexpression (*SI Appendix*, Fig. S12*E*). We observed type III signals, which occurred within 3- to 4.5-s interval from approach to sniffing, in EphB2 overexpressing group (*SI Appendix*, Fig. S12*F*). The proportions of types II and III calcium signal in EphB2 overexpressing group were increased, while the proportion of the type I was decreased (*SI Appendix*, Fig. S12*G*). These results reveal that overexpression of EphB2 increases the activation of dmPFC neurons preceding approach, but not to sniffing, thus restoring the ability of the mice for long-range social approach.

Partner dmPFC Activity Is Responsive Timely to Approaching Mice for Social Interaction. We next asked whether the brain activity of the social partner is responsive to the approaching subject mouse. We recorded calcium signals in dmPFC from two social individuals simultaneously during the reciprocal social interaction and found an obvious neural correlation in WT-partner paired group during either approach or sniffing epoch, which were much higher than that of EphB2 KI-partner paired group, and the difference was completely eliminated by social segregation (Fig. 3*A*, *SI Appendix*, Fig. S13, and Movies S2 and S3), indicating that the interaction with social partner rather than environmental sensory input determines the relevance of neural activities. We then analyzed the responsive behavior of the partner mice and the changes of partner's dmPFC neuronal activity in detail as well in each single social approach or sniffing event in reciprocal social interaction. We found that the WT partners spent longer time in the interaction zone than the EphB2 KI partners, and the area under the curve and peak value of calcium signal were significantly lower in partner of EphB2 KI mice than that of WT mice during approach epochs, while they showed no such changes during sniffing epochs (Fig. 3 *B*–*E*).

To analyze the behavioral trial precisely, we divided the calcium signals of the two mice into three categories according to their Pearson's correlation coefficients (PCC) for both WT-partner paired group and EphB2 KI-partner paired group: correlated (>0.7), partially correlated (0.3 to 0.7), and uncorrelated (<0.3) (Fig. 3*F*). We quantified the categories of pairs according to Type I/II and Type III/IV of social approach, and found an increase in percentage of uncorrelated pairs and a decrease in correlated pairs in EphB2 KI paired group, though no difference was seen between the types of social approach in WT paired group (Fig. 3*G*). The mean PCC level was not altered either in EphB2 KI paired group compared with WT paired group (Fig. 3*H*). To further determine the time lag of dmPFC activity for reciprocal social interaction, we calculated the time intervals of approach calcium peak between subject WT/KI mice and their partners. We found that although the time lag remained unchanged within each category between two paired groups, the percentage of correlated interbrain activity was altered: 83% of the time interval in WT paired group was in the range of 0 to 1.5 s, while only 54% of the time interval in EphB2 KI paired group (Fig. 3*I*), suggesting that Q858X mutation impedes interbrain activity coherence. These results indicate that EphB2 function is also required in the interbrain association of neuronal activity between the approaching mice and their social partners.

Interbrain Synchronous Activation of dmPFC Neurons Promotes Social Interaction. We then selectively enhanced the activity correlation of dmPFC neurons during social contact by using AAV-Syn-ChR2-mCherry to deliver channelrhodopsin-2 (ChR2) into dmPFC neurons to test whether synchronous activation of dmPFC neurons in EphB2 KI paired group is sufficient to rescue social behavior (Fig. 4*A* and *SI Appendix*, Fig. S14). On the basis of previous researches (20), we used identical stimulation pattern for both social individuals to trigger synchronous interbrain activity (0/2/5/10 Hz stimulation), while asynchronous activity across social animals was generated through employing different stimulation patterns (0/2/5/10 Hz versus 25 Hz stimulation) (Fig. 4 *B* and *C*). In order to couple stimuli with social interaction, we used a software to trigger the photogenetic device to deliver in vivo stimulation when the software recognized that the EphB2 KI mice had entered the non-social area (Fig. 4*B* and *D*). The ability of dmPFC neurons to follow selected stimulation patterns was validated by using in vitro current-clamp recordings of dmPFC neurons, with temporally matched optical activation using 460-nm laser (Fig. 4*E*). We observed that the duration of social interaction between EphB2 KI mice and their partners was significantly increased when the dmPFC neurons in both social animals were optogenetically stimulated in a synchronized pattern at 5 and 10 Hz rather than 2 Hz, but it remained unchanged when desynchronized or unpaired stimulation at 2 and 5 Hz was delivered to social individuals during social interaction (Fig. 4*F*). We analyzed the duration into interaction zone of subject and partner under 10 Hz activation, and found that the stimulation with synchronous pattern increased the amount of time that subjects and their partners spent in the area of interaction, whereas the asynchronous pattern drove only subjects, but not partners, into the area of interaction (Fig. 4 *G* and *H* and Movie S4). We then investigated whether the activated dmPFC could trigger

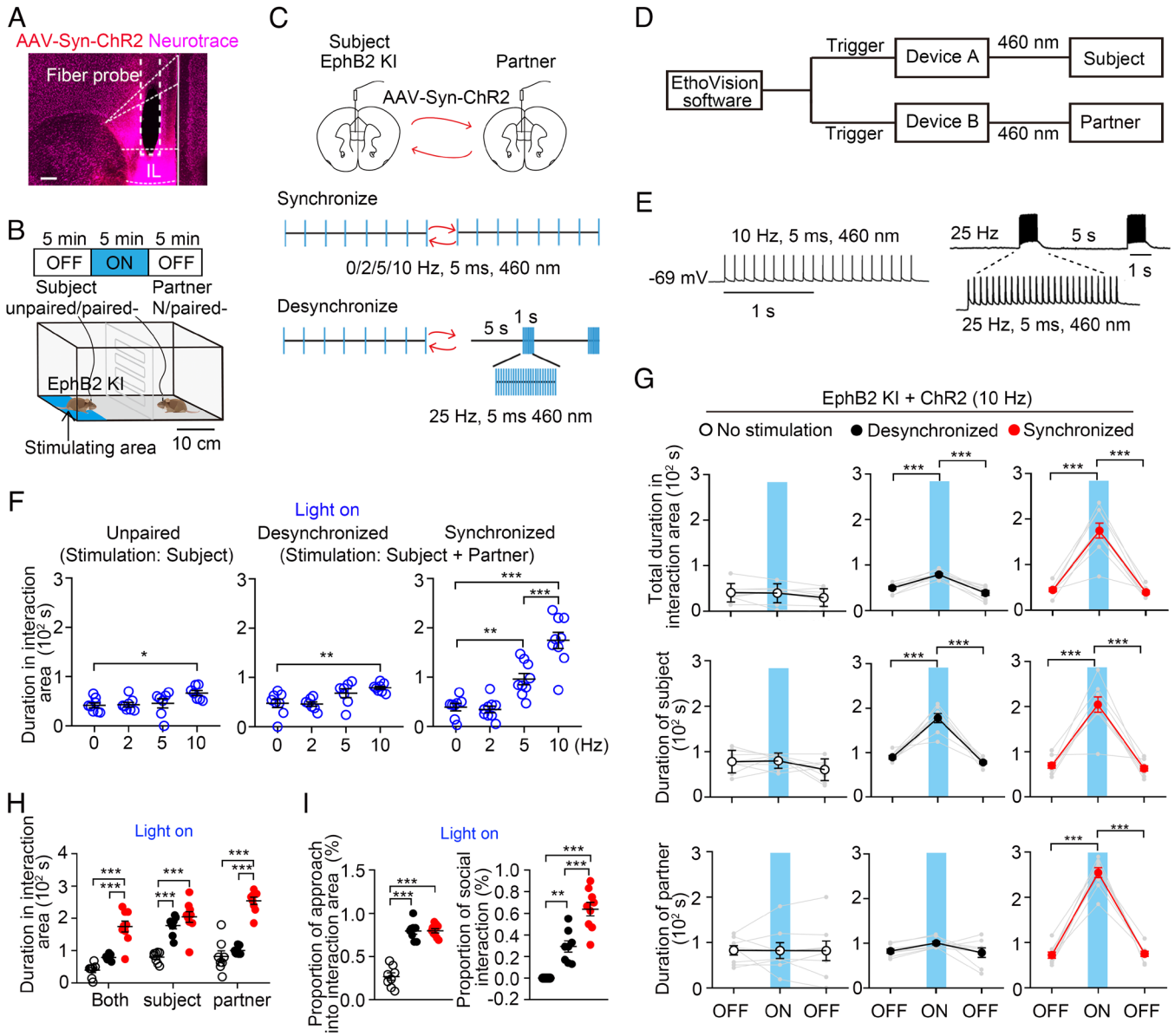

Fig. 4. Synchro-optogenetic Activation of dmPFC Rescues Social Defects in EphB2 KI Mice. (*A*) Example image illustrating the optical fiber placement and ChR2-expressing region in the dmPFC. (*B*) Schematic of laser delivery strategy during reciprocal social interaction paradigm. Blue, laser on. N, no stimulation. (*C*) Schematic showing the patterns of synchronized or desynchronized strategy. (*D*) Schematic of software-triggered laser delivery strategy. (*E*) Whole cell recording showing that dmPFC neurons exhibit various activation in response to synchronized (*Left*) and desynchronized (*Right*) activation. (*F*) Duration in interaction area during unpaired or paired (synchronized/desynchronized) activation. (*G*) Duration in interaction area of both social individuals, subjects or their partners at 10 Hz stimulation were calculated, respectively. Blue, laser on. (*H*) Summary the duration of both social individuals, subjects and their partners spending in the interaction area at 10 Hz stimulation, respectively. (*I*) The proportion of approach into interaction area (*Left*) or social interaction (*Right*) was calculated for three groups. n = 7 to 8 mice for unpaired stimulation group, n = 7 to 8 mice for desynchronize group and n = 8 to 9 mice for synchronize group, the number of partner mice was the same as that of the subjects. Data are presented as mean ± SEM. **P* < 0.05; ***P* < 0.01; ****P* < 0.001; one-way ANOVA with Tukey's multiple comparisons test (*F*, *G*, and *I*); two-way ANOVA with Tukey's multiple comparisons test (*H*).

approach behavior through measuring the proportion of EphB2 KI mice that entered the interaction area within 2 s of light activation and the proportion of social sniffing that occurred within the interaction zone (Fig. 4*I* and Movie S4). We found that although either synchronous or asynchronous activation of dmPFC in EphB2 KI mice increased the rate of social areas entry comparably, synchronous activation increased the ratio of social sniffing with their partner more dramatically than other groups (Fig. 4*I* and Movie S4).

We then asked whether the increased neural correlation across EphB2 KI mice and partner could induce a social preference in the three-chamber paradigm upon unpaired and paired (synchronized/ desynchronized) stimulation. We put strange partner mice in the cages of both sides of the chamber, named partner 1 and partner 2. We optogenetically stimulated only the EphB2 KI mouse itself when it approached partner 1, whilst costimulated the EphB2 KI mouse and partner 2 when it approached the partner 2 (Fig. 5*A*). We found that EphB2 KI mice preferred to stay with partner 2 in which the dmPFC neurons were activated in a synchronized pattern at 5 and 10 Hz, while the preference remained unchanged when desynchronized stimulation (with partner 2) or unpaired stimulation (with partner 1) was delivered during social interaction (Fig. 5 *B*–*D*).

Finally, we examined more closely how the social preference of subject mouse for its partner occurred and whether behavioral responses of the partner were inducible during the synchronous

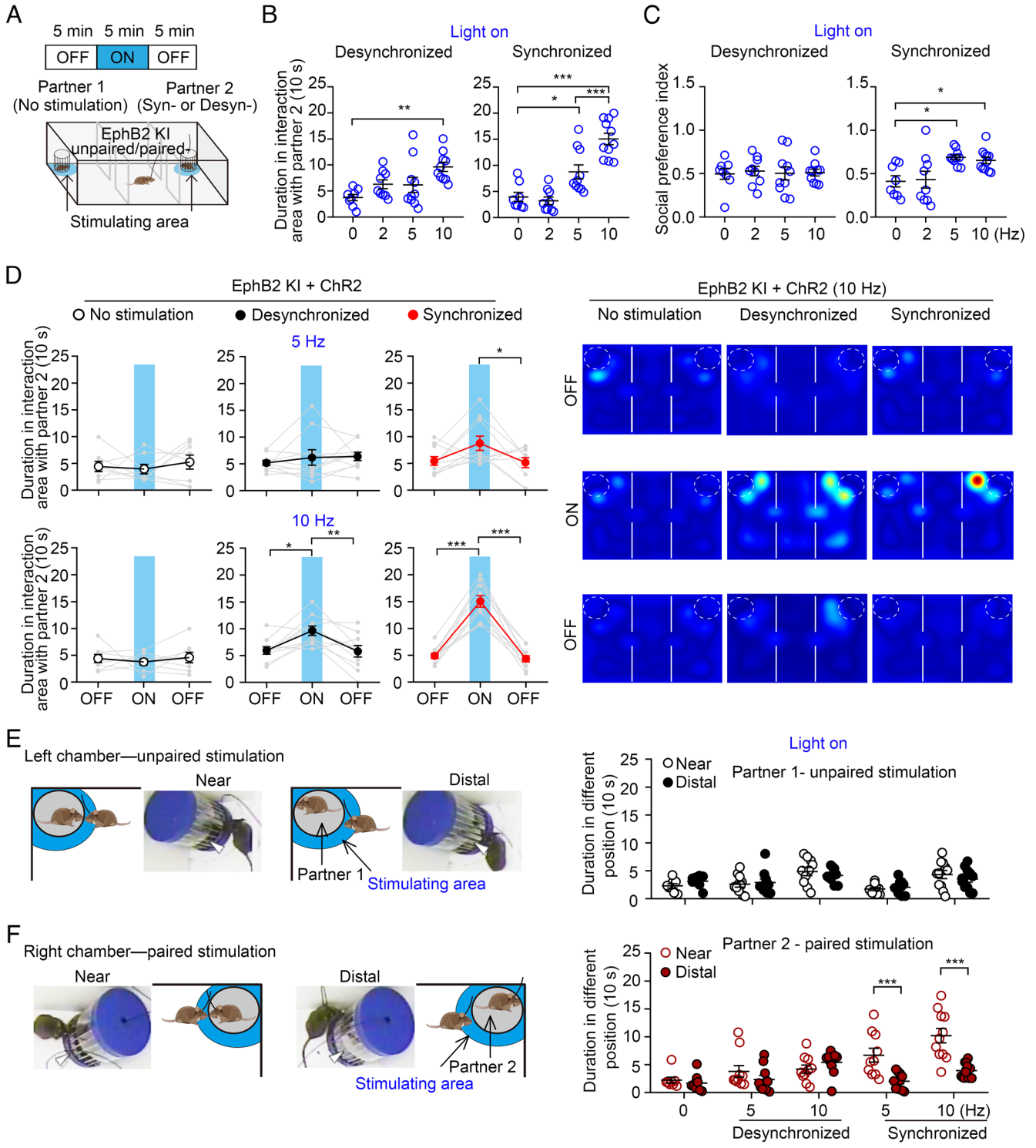

Fig. 5. Synchro-optogenetic Activation of dmPFC Induces Social Preference in EphB2 KI Mice. (*A*) Schematic of laser delivery strategy during three-chamber test. Blue, laser on. (*B*) The duration in interaction area was calculated during optical stimulation. (*C*) Social preference index was measured during optical stimulation. (*D*) The duration in interaction area with partner 2 was calculated at 5 or 10 Hz stimulation (*Left*). Heatmap of three-chamber test at 10 Hz stimulation (*Right*). (*E*) Schematic of partner 1's two position during optical stimulation (*Left*). The duration of partner 1 at near or distal position during unpaired stimulation of subject (*Right*). (*F*) Schematic of partner 2's two position during optical stimulation (*Left*). The duration of partner 2 at near or distal position during paired stimulation of subject and partner (*Right*). n = 8 to 11 mice for per group. The number of partner mice was twice as that of the subjects. Data are presented as mean ± SEM. $^{*}P < 0.05$; $^{**}P < 0.01$; $^{***}P < 0.001$; one-way ANOVA with Tukey's multiple comparisons test (*B* and *C*), two-way ANOVA with Tukey's multiple comparisons test (*D*) and two-way ANOVA with Sidak's multiple comparisons test (*E* and *F*).

activation of dmPFC. To figure this out, we deciphered the responsive interacting behaviors of partner mice in the cage upon unpaired or paired stimulation. We classified the partner behaviors in the cage into two states: One was in the outside and close to the subject for social interaction (near-position); the other was located inside and far away from the subject to socialize (distal position, Fig. 5 *E* and *F*). We observed that partner 2 spent longer time in the near position to interact with the subject mice than that in distal position upon synchronous stimulation, whereas the duration was unchanged upon either unpaired simulation (partner 1) or desynchronized stimulation

(partner 2) (Fig. 5 *E* and *F* and Movie S5). Together, these results demonstrate that intermouse synchronous activity of dmPFC neurons promotes the social behaviors, and EphB2 is essential for the activity of dmPFC across mice while they encounter their social partners.

Discussion

Most social animals establish social interactions aiming to transmit value information across peers and generations, in which individuals need to understand social rules within groups, and process postural information to further infer a peer's identity, potential actions, social hierarchy and emotional state (4, 21–23). In this study, we find that social approach, an initial stage of social actions, is compromised in EphB2 KI mice with autism-associated de novo Q858X mutation that leads to decreased sociability. We identify dmPFC, rather than other key areas of social brain, as an integrative center responding to the social partner, and further clarify the timing of neuronal activation in the dmPFC region, which precedes approach process in WT mice rather than that in EphB2 KI mice. Interestingly, we discover that the dmPFC activity in partner is inducible and correlated with approaching mice in EphB2-dependent manner (Fig. 3). This finding is distinct to not only extensive studies about roles of EphB2 in synaptic plasticity and learning/memory-based cognitive function (16), but also our previous work on social memory that occurs merely in hippocampus (17). The study thus indicates critical roles of the flexible approach with variable distance to process dynamic information that may help to guide appropriate decision for social behavior.

The dmPFC neurons are necessary in the control of autonomous and adaptive action choices, reward processing, and decision formation through encoding social information about emotion, familiarity, gender, or dominance of social partners (23–31). Given the ambiguous evidence on either enhanced (32) or weakened activity (33) of local dmPFC neurons in social disorders, how local dmPFC neurons mediate initial social interactions remains controversial. Our results reveal that dmPFC neurons are activated for the processes of both approach and thereby sniffing with partners. In particular, the response of dmPFC neurons to the partner lasts longer and occurs more diversely prior to the social contact in WT mice than in EphB2 KI mice. This indicates that the dmPFC neurons might be capable of holding information for some time during detection stage before behavioral onset, which may account for the diversity of calcium signals in WT dmPFC neurons. This assumption on dmPFC dependent long-range approach is consistent with previous study that PFC cells remain continuously active to maintain specific messages even when motor choices have not been made (25). These evidences indicate that the frontal cortex is responsible for constructing more abstract, task-relevant higher-order information, which is distinct to the function of encoding detailed and specific lower-order information, allowing rodent brain to flexibly respond to the complex and changing environment.

Moreover, we find that the timing of neuronal activation in dmPFC is positively correlated to the approach distance, and their partners also exhibit timely correlated dmPFC activity, which is seen obviously in WT paired group but not in EphB2 KI paired group. These results suggest that dmPFC might mediate distinct social approach strategies: the flexible approach requires EphB2 to sustain a proactive dmPFC activity and initiate social interaction with their partners, while the stereotyped approach is independent of EphB2 but exhibits a rigid neuronal activity that can not induce responsiveness from their partner's brain. Considering that behavioral interaction can be viewed as an interaction between two brains, we further perform interbrain synchronous activation of both social individuals, EphB2 KI and its partner, and rescues their social defects in the behavioral test, which ultimately contributes to a social preference in partner selection. These results indicate that synchronous brain activities across social animals play a crucial role in reciprocal interaction required for the sociability. In line with this view, it has been reported that the feedback from social partners affected the subject's social decision-making which was critical for social interactions (6, 34–36).

EphB2 receptor has been demonstrated to regulate neural activity in cortical neurons (37). Consistently, we find that EphB2 deficiency results in impaired inducible activity of dmPFC neurons. As a postsynaptic tyrosine receptor kinase, EphB2 is able to bind NMDA receptor on the cell membrane and transduce intracellular signaling to potentiate calcium flux (37–39), which is further validated by our present immunoblotting data that EphB2 mutation leads to downregulation of expression and function of NMDA/AMPA receptors in PFC. Furthermore, the EphB2 KI mice exhibit stereotyped social behaviors, with short duration for either approach or sniffing, which may result from the disrupted calcium flux in dmPFC. This presumption is validated by overexpression of EphB2 in the dmPFC of EphB2 KI mice in which both the calcium signal during social approach and the sociability are restored. In addition to the autism spectrum disorders (14, 15), EphB2 signal deficit has also been found in patients of anxiety disorders (40), Angelman syndrome (41), and cognitive dysfunction (18, 42), brain disorders accompanied by various social abnormality, therefore indicating a common molecular basis of social brain function.

Accumulating evidence indicates that prefrontal cortex-related circuits exert an important role in social behavior (43–46). The effects of dmPFC downstream loops and upstream inputs in social approach differ in predicting and quantifying social behaviors. Although the present findings do not reveal how the dmPFC responds to social stimuli at the level of neural circuits during the dynamic social behavior, the results indicate that timed and correlated responsiveness in brain activity from social animals is necessary and sufficient to initiate and affect behavior. In conclusion, the study provides a novel elucidation for the significant correlation between the flexible social approach and the sociability that requires the function of EphB2 signaling. This would lead to a better understanding of how PFC neuronal activity is dysregulated in the autism brain to compromise social behaviors, and bring about new insight for the treatment of these social brain disorders.

Materials and Methods

Refer to *SI Appendix* for stereotaxic surgery, activity-dependent labeling strategy, tests for olfactory and visual function, immunohistochemistry, biochemistry and western blotting, RNAscope assay, and in vitro electrophysiology.

Mice. *EphB2*$^{-/-}$ (47) mice were in 129 background and were genotyped as reported. All procedures for animal care and use were performed at an Association for Assessment and Accreditation of Laboratory Animal Care approved Facility at the Shanghai Jiao Tong University School of Medicine. Adult mice (2 to 3 mo old) were used for experiments. Behavioral experiments were carried out during the animals' light cycle.

Generation of the *EphB2* Point Mutant Mice. The *EphB2* targeting vectors used incorporated *loxP* site-specific recombination sequences and were designed to generate two-step mutations as described previously (48) from a single gene targeting event in mouse embryonic stem cells. For detailed methods, refer to *SI Appendix*.

Behavioral Assays. For the three-chamber test, the subject mice and partner mice were both habituated to the three-chamber apparatus for 10 min the day before experiment. On the test day, mice were allowed to explore freely for 10

min in the three-chamber apparatus interacting with partner or empty cage. For reciprocal social behavioral test, all animals were acclimated to the two-chamber apparatus and cable for 10 min per day for three consecutive days. On the test day, two animals were simultaneously placed in the two-chamber to explore freely for 10 min with social partner. All the behavioral videos were captured and analyzed by EthoVision XT 15 software. For detailed methods, refer to *SI Appendix*.

Fiber Photometry Recording. Adult mice were injected with AAV2/9-hSyn-GCaMP6s into the dmPFC of EphB2 KI mice and their partners followed by optical fiber implantation 2 to 3 mo postnatally. We recorded two animals' dmPFC activity simultaneously in interaction/segregation paradigm and another 10 min interaction paradigm for detailed analysis during each behavior session. For detailed methods, refer to *SI Appendix*.

In vivo Optogenetic Manipulations in Behavioral Test. In the rescue optical stimulation experiment, we connected the laser to a path cord, which was connected through a fiber optic rotary joint avoiding entanglement of optical fiber. The optogenetic manipulation protocol was carried out as previously reported (20). To verify the function of AAV2/9-hSyn-ChR2-mCherry virus, we injected ChR2 in dmPFC neurons and recorded the action potentials of mCherry-expressing neurons under light stimulation. To activate ChR2-expressing neurons of dmPFC, tonic light pulses at 2/5/10 Hz or bursting light pulses at 25 Hz (1-s-long burst every 5 s) were delivered. In the behavioral test, light activation is automatically triggered when the subject enters the stimulating area, and the time spent in areas of social contact was automatically recorded by using Noldus software. For detailed methods, refer to *SI Appendix*.

Statistical Analysis All data are presented as means ± SEM except otherwise specified. Statistical analyses were determined by using Prism 8 (GraphPad). Behavior experiments was video recorded and analyzed by using EthoVision XT 15 (Noldus). Statistical differences were conducted with Student's *t* test for two-group comparisons or ANOVA for multiple comparisons with more than two groups.

Data, Materials, and Software Availability. All study data are included in the article and/or *SI Appendix*.

ACKNOWLEDGMENTS. This research was supported by the STI2030-Major Projects (no. 2021ZD0202801 to N.-J.X.), the National Natural Science Foundation of China (32030042 and 81870820 to N.-J.X., 81970997 to S.S.), and State Key Laboratory of Neuroscience (Grant No. SKLN -2019B01). This study also was supported by Shanghai Frontiers Science Center of Cellular Homeostasis and Human Diseases.

Author affiliations: [a]Research Center of Translational Medicine, Shanghai Children's Hospital, Department of Anatomy and Physiology, Shanghai Jiao Tong University School of Medicine, Shanghai 200062, China; [b]Songjiang Institute, Songjiang District Central Hospital, Shanghai Jiao Tong University School of Medicine, Shanghai 201699, China; [c]Department of Neurology and Institute of Neurology, Rui Jin Hospital, Shanghai Jiao Tong University School of Medicine, Shanghai 200025, China; [d]Institute of Neuroscience and State Key Laboratory of Neuroscience, Center for Excellence in Brain Science and Intelligence Technology, Chinese Academy of Sciences, Shanghai 200031, China; [e]Shanghai Key Laboratory of Reproductive Medicine, Shanghai Jiao Tong University School of Medicine, Shanghai 200025, China; and [f]Key Laboratory of Cell Differentiation and Apoptosis of Chinese Ministry of Education, Shanghai Jiao Tong University School of Medicine, Shanghai 200025, China

1. K. Hashikawa, Y. Hashikawa, A. Falkner, D. Lin, The neural circuits of mating and fighting in male mice. *Curr. Opin. Neurobiol.* **38**, 27–37 (2016).
2. D. Wei, V. Talwar, D. Lin, Neural circuits of social behaviors: Innate yet flexible. *Neuron* **109**, 1600–1620 (2021).
3. J. E. LeDoux, Evolution of human emotion: A view through fear. *Prog. Brain Res.* **195**, 431–442 (2012).
4. J. P. Mitchell, Social psychology as a natural kind. *Trends Cogn. Sci.* **13**, 246–251 (2009).
5. N. Tinbergen, Derived activities; their causation, biological significance, origin, and emancipation during evolution. *Q Rev. Biol.* **27**, 1–32 (1952).
6. P. Chen, W. Hong, Neural circuit mechanisms of social behavior. *Neuron* **98**, 16–30 (2018).
7. L. Kingsbury *et al.*, Correlated neural activity and encoding of behavior across brains of socially interacting animals. *Cell* **178**, 429–446 e416 (2019).
8. C. Dulac, A. T. Torello, Molecular detection of pheromone signals in mammals: From genes to behaviour. *Nat. Rev. Neurosci.* **4**, 551–562 (2003).
9. T. R. Insel, R. D. Fernald, How the brain processes social information: Searching for the social brain. *Annu. Rev. Neurosci.* **27**, 697–722 (2004).
10. J. T. Winslow, F. Camacho, Cholinergic modulation of a decrement in social investigation following repeated contacts between mice. *Psychopharmacology* **121**, 164–172 (1995).
11. J. Peca *et al.*, Shank3 mutant mice display autistic-like behaviours and striatal dysfunction. *Nature* **472**, 437–442 (2011).
12. N. Hahn *et al.*, Monogenic heritable autism gene neuroligin impacts Drosophila social behaviour. *Behav. Brain Res.* **252**, 450–457 (2013).
13. O. Penagarikano *et al.*, Absence of CNTNAP2 leads to epilepsy, neuronal migration abnormalities, and core autism-related deficits. *Cell* **147**, 235–246 (2011).
14. A. Kong *et al.*, Rate of de novo mutations and the importance of father's age to disease risk. *Nature* **488**, 471–475 (2012).
15. S. J. Sanders *et al.*, De novo mutations revealed by whole-exome sequencing are strongly associated with autism. *Nature* **485**, 237–241 (2012).
16. N. T. Henderson, M. B. Dalva, EphBs and ephrin-Bs: Trans-synaptic organizers of synapse development and function. *Mol. Cell Neurosci.* **91**, 108–121 (2018).
17. X. D. Liu *et al.*, Hippocampal Lnx1-NMDAR multiprotein complex mediates initial social memory. *Mol. Psychiatry* **26**, 3956–3969 (2021).
18. X. R. Wu *et al.*, EphB2 mediates social isolation-induced memory forgetting. *Transl. Psychiatry* **10**, 389 (2020).
19. A. Assali, J. Y. Cho, E. Tsvetkov, A. R. Gupta, C. W. Cowan, Sex-dependent role for EPHB2 in brain development and autism-associated behavior. *Neuropsychopharmacology* **46**, 2021–2029 (2021).
20. Y. Yang *et al.*, Wireless multilateral devices for optogenetic studies of individual and social behaviors. *Nat. Neurosci.* **24**, 1035–1045 (2021).
21. P. A. Brennan, K. M. Kendrick, Mammalian social odours: Attraction and individual recognition. *Philos Trans. R. Soc. Lond. B Biol. Sci.* **361**, 2061–2078 (2006).
22. C. V. Portfors, Types and functions of ultrasonic vocalizations in laboratory rats and mice. *J. Am. Assoc. Lab. Anim. Sci.* **46**, 28–34 (2007).
23. T. Zhou *et al.*, History of winning remodels thalamo-PFC circuit to reinforce social dominance. *Science* **357**, 162–168 (2017).
24. K. K. Cho *et al.*, Gamma rhythms link prefrontal interneuron dysfunction with cognitive inflexibility in Dlx5/6(+/-) mice. *Neuron* **85**, 1332–1343 (2015).
25. C. H. Donahue, D. Lee, Dynamic routing of task-relevant signals for decision making in dorsolateral prefrontal cortex. *Nat. Neurosci.* **18**, 295–301 (2015).
26. P. Gangopadhyay, M. Chawla, O. Dal Monte, S. W. C. Chang, Prefrontal-amygdala circuits in social decision-making. *Nat. Neurosci.* **24**, 5–18 (2021).
27. L. Kingsbury *et al.*, Cortical representations of conspecific sex shape social behavior. *Neuron* **107**, 941–953.e947 (2020).
28. A. F. Arnsten, Stress signalling pathways that impair prefrontal cortex structure and function. *Nat. Rev. Neurosci.* **10**, 410–422 (2009).
29. F. Wang *et al.*, Bidirectional control of social hierarchy by synaptic efficacy in medial prefrontal cortex. *Science* **334**, 693–697 (2011).
30. H. Xu *et al.*, A disinhibitory microcircuit mediates conditioned social fear in the prefrontal cortex. *Neuron* **102**, 668–682.e665 (2019).
31. J. H. Lui *et al.*, Differential encoding in prefrontal cortex projection neuron classes across cognitive tasks. *Cell* **184**, 489–506.e426 (2021).
32. O. Yizhar *et al.*, Neocortical excitation/inhibition balance in information processing and social dysfunction. *Nature* **477**, 171–178 (2011).
33. M. T. Lazaro *et al.*, Reduced prefrontal synaptic connectivity and disturbed oscillatory population dynamics in the CNTNAP2 model of autism. *Cell Rep.* **27**, 2567–2578.e2566 (2019).
34. J. K. Rilling, A. G. Sanfey, The neuroscience of social decision-making. *Annu. Rev. Psychol.* **62**, 23–48 (2011).
35. L. Kingsbury, W. Hong, A multi-brain framework for social interaction. *Trends Neurosci.* **43**, 651–666 (2020).
36. D. Kliemann, R. Adolphs, The social neuroscience of mentalizing: Challenges and recommendations. *Curr. Opin. Psychol.* **24**, 1–6 (2018).
37. M. A. Takasu, M. B. Dalva, R. E. Zigmond, M. E. Greenberg, Modulation of NMDA receptor-dependent calcium influx and gene expression through EphB receptors. *Science* **295**, 491–495 (2002).
38. M. B. Dalva *et al.*, EphB receptors interact with NMDA receptors and regulate excitatory synapse formation. *Cell* **103**, 945–956 (2000).
39. M. J. Nolt *et al.*, EphB controls NMDA receptor function and synaptic targeting in a subunit-specific manner. *J. Neurosci.* **31**, 5353–5364 (2011).
40. B. K. Attwood *et al.*, Neuropsin cleaves EphB2 in the amygdala to control anxiety. *Nature* **473**, 372–375 (2011).
41. S. S. Margolis *et al.*, EphB-mediated degradation of the RhoA GEF Ephexin5 relieves a developmental brake on excitatory synapse formation. *Cell* **143**, 442–455 (2010).
42. M. Cisse *et al.*, Reversing EphB2 depletion rescues cognitive functions in Alzheimer model. *Nature* **469**, 47–52 (2011).
43. M. L. Smith, N. Asada, R. C. Malenka, Anterior cingulate inputs to nucleus accumbens control the social transfer of pain and analgesia. *Science* **371**, 153–159 (2021).
44. W. C. Huang, A. Zucca, J. Levy, D. T. Page, Social behavior is modulated by valence-encoding mPFC-amygdala sub-circuitry. *Cell Rep.* **32**, 107899 (2020).
45. B. Xing *et al.*, A subpopulation of prefrontal cortical neurons is required for social memory. *Biol. Psychiatry* **89**, 521–531 (2021).
46. E. Kelly *et al.*, Regulation of autism-relevant behaviors by cerebellar-prefrontal cortical circuits. *Nat. Neurosci.* **23**, 1102–1110 (2020).
47. M. Henkemeyer *et al.*, Nuk controls pathfinding of commissural axons in the mammalian central nervous system. *Cell* **86**, 35–46 (1996).
48. N. J. Xu, M. Henkemeyer, Ephrin-B3 reverse signaling through Grb4 and cytoskeletal regulators mediates axon pruning. *Nat. Neurosci.* **12**, 268–276 (2009).